

CALCULATED POWDER PATTERNS: I. FIVE PLAGIOCLASES

I. Y. BORG AND D. K. SMITH, *Lawrence Radiation Laboratory
University of California, Livermore, California.*

ABSTRACT

As an aid in indexing complex plagioclase X-ray powder patterns, integrated (I_{INT}) and peak (I_P) intensities are calculated for five plagioclases [low and high albite (An_0), oligoclase (An_{29}), bytownite (An_{90}) and anorthite (An_{100})]. Lorentz-polarization, absorption and multiplicity corrections appropriate to powder mounts are applied to temperature-corrected $|F|^2$ which are calculated from single-crystal structure analyses. Graphical expression of I_P as a function of 2θ results in plots which are very similar to the comparable experimental X-ray diffraction traces.

PREAMBLE

X-ray diffraction data are indispensable in modern studies of the plagioclase feldspars. Extensive studies relating lattice parameters to composition and conditions of crystallization have laid the basis for advanced studies on the relation of feldspars to other minerals. Many studies involve the use of x-ray powder patterns and require the reduction of complex patterns to yield the unit-cell dimensions. The assignment of Miller indices, hkl , to the observed diffraction maxima to obtain data for a least-squares refinement is a usual step in the data reduction process. The low symmetry of the plagioclases, their pseudo-symmetry (low obliquity), and rather large unit cells result in powder patterns of closely spaced and overlapped maxima. Because of rapid changes in cell constants with composition, as well as small changes in intensity related to composition, atomic distribution (disorder) and atomic coordinates, reliable and general guides to correct indexing, are precluded. For example, separating the approximately 120 reflections with intensities greater than 2 in the first 65° , 2θ range of anorthite is virtually impossible with only approximate cell dimensions and the spacings calculated from them. Intensity data are necessary to identify the reflections that contribute to each observed maximum. Such intensity data may be obtained from careful study of a series of powder patterns over the whole compositional and disorder range; however, some question usually remains as to the correct identity of some lines.

A better guide to relative hkl intensities is structure factors conventionally tabulated in descriptions of single-crystal structure analyses. For complex structures like the feldspars these tables are generally too numerous for publication, and are only available upon specific request to the investigators. Even when such tables are in hand, for the purpose of comparison with powder data, they must be interpreted in terms of the

absorption, Lorentz-polarization, and multiplicity corrections applicable to powder samples. Therefore, in order to put the data from structure analyses in a more convenient form for use with powder patterns, sets of X-ray intensities have been calculated for five plagioclases.

SOURCE OF DATA FOR CALCULATIONS

The five plagioclases for which powder patterns have been calculated include low and high albite, An_0 (Ribbe, Megaw, and Taylor, 1968); oligoclase, An_{29} (Colville and Ribbe, 1966); bytownite "body-centered anorthite," An_{80} (Fleet, Chandrasekhar, and Megaw, 1966); and anorthite, An_{100} (Kempster, Megaw, and Radoslovich, 1961). Results of calculations for transitional anorthite, An_{99} (Ribbe and Megaw, 1963) are not tabulated because of their similarity to those of anorthite; however, a calculated pattern is displayed for comparison. The chief difference in the two structures lies in the presence of sharp, very weak "d" reflections, and sharp, medium strong "c" reflections in anorthite. A resumé of pertinent parameters is given in Table 1. Minor K, Na, and Ca were generally ignored in the structural refinements and, as a consequence, the albites and anorthite were treated as pure $NaAlSi_3O_8$ and $CaAl_2Si_2O_8$, respectively, in results of calculations presented here. A random distribution was assumed on the Na/Ca sites for oligoclase and bytownite. All data were derived from three-dimensional structure analyses.

CALCULATIONS

The calculated intensities and spacings tabulated in Tables 2-7 were calculated from Smith's (1967, 1968) program for calculating powder diffraction patterns. Required input data include unit-cell dimensions, space group, atomic coordinates including site occupancy, temperature factors, and atomic scattering factors. If absorption corrections appropriate to the shape of the shape (in this case a cylinder or flat plate) are to be applied, linear absorption coefficients or density, atomic weights, and mass absorption coefficients are also needed. After a temperature-corrected $|F|^2$ is calculated, multiplicity, Lorentz-polarization corrections, and absorption factors are applied to give an integrated intensity for each hkl reflection permitted by the space group.

The decision to calculate structure factors rather than use published values of $|F_{obs}|$ or $|F_{calc}|$ is in consideration of the voluminous amount of input and attendant errors that are thereby eliminated. Agreement between $|F_{calc}|$ generated by the program and $|F_{calc}|$ published by the original researchers is a convenient check on the accuracy of the input used to generate the calculated powder intensities.

The calculated integrated intensity (I_{INT}) is directly proportional to the total energy per unit time for each diffraction event, and is independent of instrumental errors and

TABLE 1. DESCRIPTION OF PLAGIOCLASES

Variety Composition	Low Albite Ab _{98.5} An _{0.5} - Or _{1.3}	High Albite Ab _{97.7} An _{0.7} - Or _{1.6}	Oligoclase Ab ₆₉ An ₂₉ - Or ₂	Bytownite ~Ab ₂₀ An ₈₀	Anorthite ~Ab ₀ An ₁₀₀	
Source	Ramona, Calif.	Amelia, Va. (Inverted from low form)	Mitchell Co., N. C.	St. Louis Co., Minn.	Monte Somma, Italy	
<i>a</i> (Å)	8.138	8.149	8.169	8.178	8.1768	
<i>b</i>	12.789	12.880	12.851	12.870	12.8768	
<i>c</i>	7.156	7.106	7.124	14.187	14.1690	
α (deg)	94.33°	93.37°	93.63°	93.50°	93.17°	
β	116.57°	116.30°	116.40°	115.90°	115.85°	
γ	87.65°	90.28°	89.46°	90.63°	91.22°	
Space group	C1	C1	C1	I1	P1	
Site occupancy (% Si)						
T ₁ (0)	(0000)	0 ^a	72 ^a	35	100	100
	(00i0)				100	100
	(0z00)	0	72	35	6	0
	(0zi0)				0	0
T ₁ (m)	(m000)	100	75	81	13	0
	(m0i0)				13	0
	(mz00)	100	75	81	100	100
	(mzi0)				100	100 ^b
T ₂ (0)	(0000)	100	78	79	30	0
	(00i0)				13	0
	(0z00)	100	78	79	100	100
	(0zi0)				100	100
T ₂ (m)	(m000)	100	75	81	100	100
	(m0i0)				90	100 ^b
	(mz00)	100	75	81	13	0
	(mzi0)				13	0
<i>R</i>	0.068	0.082	0.069	0.118	0.111	
Reference	Ribbe <i>et al.</i> (1968) Ferguson <i>et al.</i> (1958)	Ribbe <i>et al.</i> (1968) Ferguson <i>et al.</i> (1958)	Colville & Ribbe (1966)	Fleet <i>et al.</i> (1966)	Kempster <i>et al.</i> (1962); Megaw <i>et al.</i> (1962); Cole <i>et al.</i> (1951)	

^a Ribbe, personal communication, 1968.

^b These sites are reported to contain 10% Al (Megaw *et al.*, 1962, p. 1023), but because strain effects can limit the accuracy of apparent site occupancy to $\pm 5\%$, for simplicity these sites are considered to be 100% Si in subsequent calculations (Fleet *et al.* (1966) p. 797).

other aberrations. The peak intensity (I_P), on the other hand, is not so easily interpreted because it is sensitive to the real dispersion of the diffracted waves producing the maximum.

TABLE 2. CALCULATED POWDER DATA FOR LOW ALBITE (An₀)

2 θ (INT)	2 θ (P)	d	hkl	I _{INT}	I _P	2 θ (INT)	2 θ (P)	d	hkl	I _{INT}	I _P
13.86		6.387	001	7		49.97	49.98	1.825	043	5	9
13.89	13.88	6.376	020	4	9	50.00		1.824	052	7	
13.96		6.343	110	3		50.13	50.13	1.820	400	12	9
14.06		6.299	110	3		50.63	50.64	1.803	113	9	5
14.99	14.99	5.912	111	4	2	51.21	51.21	1.784	204	20	10
15.88	15.88	5.581	111	4	3	52.16		1.753	420	2	3
22.07	22.07	4.027	201	93	61	52.19	52.18	1.753	224	4	
23.08	23.08	3.854	111	15	11	52.54	52.54	1.742	442	7	4
23.56	23.56	3.777	111	39	26	53.21		1.721	242	3	
24.16	24.18	3.684	130	22	21	53.28		1.719	062	3	
24.26	24.32	3.668	131	16	34	53.32	53.32	1.718	133	3	6
24.33		3.658	130	42		53.35		1.717	441	2	
25.41	25.41	3.505	112	15	10	53.35		1.717	262	4	
25.57	25.57	3.483	221	6	5	54.44	54.44	1.685	224	4	2
26.44	26.44	3.370	112	16	10	55.09	55.09	1.667	242	4	3
27.76	27.76	3.214	202	72	58	57.84	57.84	1.594	080	2	2
27.94		3.194	002	100		58.18	58.20	1.586	353	4	3
27.99	27.96	3.188	040	66	100	58.20		1.585	424	3	
28.13		3.172	220	37		58.70	58.70	1.573	024	4	3
28.34	28.34	3.150	220	39	30	58.80		1.570	081	3	
30.14	30.14	2.965	131	25	20	59.23	59.23	1.560	351	3	3
30.23		2.956	222	16		60.41	60.46	1.532	424	2	2
30.49	30.52	2.931	022	12	19	61.50	61.48	1.508	281	4	3
30.53		2.928	041	18		61.77	61.78	1.502	533	5	3
31.25	31.25	2.862	131	15	9	63.53	63.52	1.464	280	7	5
31.50	31.50	2.840	132	4	3	63.83	63.94	1.458	063	6	4
34.00	34.00	2.637	132	11	7	63.95		1.456	280	5	
35.03	35.03	2.562	241	21	12	64.93	64.94	1.436	461	6	3
35.38	35.38	2.537	312	3	2	65.20	65.20	1.431	262	6	4
35.98	35.98	2.496	221	3	2	65.40		1.427	462	5	
36.81	36.82	2.442	241	15	9	65.48	65.42	1.425	243	4	4
36.98	36.96	2.431	151	6	5	65.60		1.423	514	2	
37.35	37.36	2.408	240	5	4	66.07	66.06	1.414	114	4	2
37.46		2.401	150	3		67.13	67.16	1.394	534	4	3
37.66		2.388	240	3		67.44	67.46	1.389	190	2	2
37.68	37.68	2.387	310	2	3	67.49		1.388	460	3	
37.80		2.380	310	3		67.90	67.90	1.380	134	4	3
38.83	38.83	2.319	331	12	7	68.06	68.04	1.377	243	3	3
39.59	39.59	2.276	113	3	2	68.57	68.37	1.372	405	4	2
40.17	40.18	2.244	331	3	2	68.92	68.92	1.362	425	4	2
41.27	41.30	2.187	042	3	5	69.51		1.352	192	5	
41.51		2.186	151	5		69.55	69.54	1.352	502	6	6
42.53	42.53	2.125	060	12	7	69.74		1.348	115	4	
42.73	42.73	2.116	151	5	5	70.00	69.98	1.344	402	7	3
43.32	43.32	2.088	313	2	2	70.73	70.73	1.332	622	2	2
43.58	43.58	2.077	241	8	4	70.97	70.97	1.328	135	4	3
44.54	44.54	2.034	241	3	1	74.00	74.00	1.281	482	5	3
45.33	45.34	2.001	401	3	2	74.85	74.84	1.268	282	5	4
45.85	45.84	1.979	061	4	3	75.76	75.74	1.256	535	3	2
47.16	47.16	1.927	222	4	2	77.98	77.98	1.225	282	5	3
48.05	48.06	1.893	422	12	7	78.31	78.30	1.221	482	4	2
48.16	48.16	1.889	351	3	8	78.91	78.91	1.213	600	4	2
48.19		1.888	222	9		81.93	81.96	1.176	316	3	2
49.28	49.28	1.849	403	13	7	82.93	82.93	1.164	353	2	2
49.49	49.49	1.842	260	4	4	85.39		1.137	640	2	1
49.83	49.98	1.830	113	2	9	85.43	85.40	1.136	154	2	
49.86		1.829	260	8		85.97	85.90	1.131	540	2	1

TABLE 3. CALCULATED POWDER DATA FOR HIGH ALBITE (An₀)

2θ (INT)	2θ (P)	d	hkl	I _{INT}	I _P	2θ (INT)	2θ (P)	d	hkl	I _{INT}	I _P
13.74	13.76	6.445	$\bar{1}10$	9	16	50.13	49.96	1.820	260	5	11
13.78		6.425	020	10		50.86	50.90	1.795	$\bar{1}70$	3	7
13.93	13.93	6.356	001	4		50.91		1.794	113	8	
15.22	15.22	5.822	$\bar{1}\bar{1}1$	6	6	51.53	51.53	1.773	$\bar{2}04$	21	14
15.69	15.70	5.648	$\bar{1}11$	6	5	52.42	52.42	1.745	242	5	5
22.04	22.04	4.032	$\bar{2}01$	100	84	52.60	52.60	1.740	420	3	3
22.90	22.90	3.884	$\bar{1}11$	23	20	52.73	52.70	1.736	$\bar{2}24$	3	3
23.71	23.72	3.752	$\bar{1}30$	45	61	53.18	53.18	1.722	062	3	3
23.73		3.750	111	30		53.42	53.54	1.715	$\bar{4}41$	3	5
24.46	24.46	3.639	130	30	28	53.55		1.711	$\bar{4}42$	6	
24.56		3.625	$\bar{1}\bar{3}1$	9		53.79	53.76	1.704	$\bar{4}42$	3	3
25.66	25.66	3.472	$\bar{1}\bar{1}2$	9	8	55.67	55.67	1.651	242	4	3
26.08	26.04	3.422	$\bar{2}21$	2	3	57.12	57.12	1.612	353	4	3
26.46	26.46	3.368	$\bar{1}12$	18	15	58.92	58.90	1.568	$0\bar{2}4$	2	3
27.68	27.74	3.223	$\bar{2}20$	43	100	60.10	60.10	1.540	351	3	3
27.77		3.212	040	68		61.17	61.17	1.515	$\bar{2}44$	2	2
27.86		3.203	$\bar{2}02$	83		62.10	62.10	1.495	$\bar{2}81$	5	4
28.08	28.08	3.178	002	100	88	62.33	62.33	1.490	$\bar{2}80$	6	5
28.54	28.54	3.127	220	35	30	62.69	62.69	1.482	$\bar{5}\bar{3}3$	4	4
29.62	29.62	3.016	$\bar{1}31$	18	14	62.93	62.93	1.477	$\bar{4}61$	5	6
30.31	30.31	2.949	0 $\bar{4}1$	22	19	63.28	63.26	1.470	$\bar{5}33$	2	3
30.52	30.52	2.929	0 $\bar{2}2$	16	15	63.52	63.52	1.465	$\bar{4}62$	2	3
30.71	30.70	2.911	$\bar{2}22$	10	10	63.87	63.87	1.457	063	5	4
31.56	31.56	2.835	131	21	17	64.15	64.15	1.452	280	5	3
31.79	31.79	2.815	$\bar{1}32$	6	6	64.84	64.84	1.438	243	4	3
33.73	33.73	2.656	$\bar{1}32$	10	7	65.41	65.41	1.427	$\bar{5}14$	3	2
35.45	35.66	2.532	$\bar{2}21$	2	23	65.89	65.90	1.418	262	3	3
35.65		2.518	$\bar{2}41$	24		66.43	66.43	1.407	$\bar{2}64$	2	3
35.68		2.516	$\bar{3}\bar{1}2$	3		66.43		1.407	114	2	
35.69		2.515	$\bar{1}\bar{1}2$	3		67.25		1.392	190	3	
35.82	35.80	2.507	$\bar{2}41$	16		67.32		1.391	441	2	
36.61	36.61	2.455	$\bar{2}40$	3	4	67.78		1.382	$\bar{1}91$	2	
36.91	36.91	2.435	221	3	3	67.80		1.382	$\bar{4}63$	3	5
37.20	37.20	2.417	$\bar{1}\bar{5}1$	3	3	67.82		1.382	$\bar{1}34$	5	
37.37	37.37	2.407	$\bar{3}10$	3	3	68.12	68.12	1.376	534	3	3
37.86	37.94	2.376	310	3	6	68.69		1.366	243	2	
37.95		2.371	240	7		68.72	68.72	1.366	460	2	5
38.22	38.22	2.354	$\bar{1}51$	2	2	68.73		1.366	405	4	
39.16	39.16	2.300	$\bar{3}31$	5	4	69.35		1.355	$\bar{6}02$	6	5
39.52	39.52	2.280	$\bar{3}31$	7	6	69.50	69.38	1.352	$\bar{1}92$	5	
39.75	39.75	2.268	$\bar{1}13$	4	3	69.72		1.349	$\bar{4}25$	2	
42.19	42.19	2.142	060	11	8	69.91	69.90	1.346	402	7	5
42.63	42.63	2.121	$\bar{2}41$	12	10	70.15		1.342	115	3	
43.01	43.01	2.103	$\bar{1}51$	5	4	71.45	71.44	1.320	$\bar{1}35$	3	3
43.21	43.20	2.093	$\bar{3}13$	3	3	73.30	73.30	1.291	$\bar{2}82$	3	3
44.96	44.96	2.016	$\bar{4}02$	3	3	75.50	75.52	1.259	$\bar{4}82$	5	4
45.18	45.18	2.007	$\bar{4}01$	3	3	75.91		1.253	$\bar{4}82$	3	3
45.61	45.61	1.989	061	5	5	75.94	75.92	1.253	$\bar{6}42$	2	
46.78	46.80	1.942	$\bar{2}22$	4	3	76.85	76.84	1.240	$\bar{5}35$	2	2
47.19	47.32	1.926	$\bar{4}22$	3	7	76.89		1.240	083	1	
47.32		1.921	$\bar{4}22$	9		78.56		1.217	442	1	
48.52	48.54	1.876	$\bar{2}60$	6	8	78.62	78.68	1.217	600	4	4
48.56		1.875	$\bar{2}22$	7		78.73		1.215	$\bar{2}82$	4	
49.35	49.35	1.847	$\bar{4}03$	11	8	82.35	82.40	1.171	316	2	2
49.69	49.70	1.835	062	4	4	82.41		1.170	084	2	
49.89		1.828	$\bar{1}13$	3		83.87	83.88	1.154	353	2	2
49.92	49.96	1.827	0 $\bar{4}3$	3	11	84.07		1.151	$\bar{6}40$	2	
49.97		1.825	400	11							

TABLE 4. CALCULATED POWDER DATA FOR OLIGOCLASE (An₂₉)

2θ (INT)	2θ (P)	d	hkl	I _{INT}	I _P	2θ (INT)	2θ (P)	d	hkl	I _{INT}	I _P
13.81	13.82	6.412	1̄10	6	5	49.87		1.829	260	5	
15.13	15.13	5.856	1̄11	4	2	49.94	49.86	1.826	043	3	11
18.98	18.98	4.675	021	3	2	50.12		1.820	262	3	
21.99	21.99	4.042	201	93	52	50.78	50.78	1.798	113	10	5
22.93	22.93	3.879	111	17	10	51.41	51.41	1.777	204	24	10
23.64	23.64	3.763	111	31	19	52.55	52.58	1.741	224	4	4
23.89	23.89	3.725	130	41	24	52.63		1.739	242	5	
24.34	24.34	3.657	130	29	18	53.11	53.14	1.724	442	8	5
24.45		3.640	131	12		53.17		1.723	062	3	
25.58	25.58	3.483	112	13	8	53.75	53.78	1.705	441	3	2
25.83	25.83	3.449	221	5	3	53.86	53.86	1.702	441	2	2
26.44	26.44	3.371	112	22	12	54.09	54.09	1.695	442	4	2
27.78		3.211	202	87		54.44	54.44	1.685	224	4	3
27.83	27.82	3.206	220	45	100	55.40	55.40	1.658	242	3	1
27.83		3.206	040	67		57.38	57.38	1.606	353	5	3
28.03	28.03	3.184	002	100	64	58.50		1.578	511	2	2
28.34	28.34	3.149	220	40	25	58.59	58.56	1.575	424	3	2
29.77	29.77	3.001	131	23	12	58.84	58.84	1.569	024	3	2
30.38	30.38	2.942	041	23	15	59.71	59.71	1.549	351	3	1
30.51	30.52	2.929	022	16	18	60.08	60.10	1.540	424	2	1
30.53		2.928	222	14		61.87	61.86	1.500	251	5	3
31.42	31.42	2.847	131	20	10	62.24	62.24	1.492	533	5	3
31.70	31.70	2.823	132	5	4	62.81	62.81	1.480	280	6	3
33.80	33.80	2.651	132	13	7	63.44	63.44	1.466	461	6	4
35.41		2.535	241	26		63.44		1.466	533	3	
35.50	35.42	2.529	312	5	14	63.81		1.459	063	5	4
35.56		2.524	221	3		63.90	63.88	1.457	280	5	
35.68		2.516	112	3		63.99		1.455	462	5	
36.08	36.08	2.489	241	17	9	64.99	64.99	1.435	243	3	2
36.72	36.74	2.447	221	3	2	65.32	65.32	1.429	514	4	2
36.89	36.90	2.436	240	3	3	65.58	65.56	1.423	262	4	2
37.12	37.12	2.422	151	4	3	66.27	66.26	1.410	114	2	2
37.39	37.39	2.405	310	3	2	67.20	67.20	1.393	190	3	2
37.69	37.70	2.386	310	3	4	67.67	67.70	1.384	534	5	3
37.70		2.386	240	6		67.82	67.80	1.382	134	5	3
39.21	39.21	2.298	331	8	4	68.40	68.52	1.371	243	3	3
39.39	39.38	2.288	331	6	3	68.54		1.369	405	5	
39.68	39.68	2.271	113	3	2	69.16	69.16	1.358	602	8	4
40.77	40.76	2.213	151	3	2	69.39	69.48	1.354	425	4	4
41.82	41.82	2.160	223	3	2	69.50		1.352	192	6	
42.29	42.29	2.137	060	10	5	69.77	69.78	1.348	402	7	3
42.88	42.88	2.109	151	7	8	70.00		1.344	115	4	
42.89		2.109	241	12		71.02	71.04	1.327	553	3	
43.18	43.16	2.095	313	4	3	71.30	71.30	1.323	135	4	3
44.84	44.86	2.021	402	3	3	73.76	73.76	1.285	282	4	2
45.08	45.08	2.011	401	3	2	74.92	74.92	1.267	482	5	5
45.66	45.66	1.987	061	4	3	76.11	76.14	1.251	643	3	2
46.85	46.86	1.939	222	3	3	76.27	76.26	1.248	642	3	2
47.41	47.41	1.917	422	13	6	76.55	76.55	1.245	482	4	2
48.37	48.37	1.882	222	8	4	78.39	78.42	1.220	282	4	3
48.91	48.91	1.862	260	6	4	78.44		1.219	600	3	
49.21	49.21	1.852	403	11	5	79.22	79.18	1.209	355	3	2
49.79	49.86	1.831	062	5	11	82.17	82.17	1.173	316	3	1
49.86		1.829	400	13		84.40	84.44	1.148	640	3	1
						84.62	84.58	1.145	265	2	1

TABLE 5. CALCULATED POWDER DATA FOR BYTOWNITE (An₈₀)

2θ (INT)	2θ (P)	d	hkl	I _{INT}	I _P	2θ (INT)	2θ (P)	d	hkl	I _{INT}	I _P
12.94	12.94	6.839	111	2	2	42.68	42.66	2.118	134	2	3
13.63	13.63	6.498	110	9	9	42.96	42.98	2.105	136	4	4
13.80	13.80	6.417	020	9	9	43.12	43.12	2.098	152	5	5
13.92		6.364	002	4		43.29	43.28	2.090	316	4	4
15.25	15.25	5.809	112	10	8	44.86		2.020	404	3	
15.71	15.71	5.640	112	5	5	44.87	44.88	2.020	154	7	8
17.65	17.65	5.026	121	2	2	44.95		2.017	402	5	
18.90	18.90	4.694	022	2	1	45.26	45.24	2.004	312	3	3
20.36	20.36	4.361	022	2	2	45.73	45.73	1.984	062	2	2
22.00	22.00	4.041	202	100	82	46.11	46.10	1.968	312	2	3
22.73	22.73	3.913	112	31	26	46.41	46.41	1.956	224	2	2
23.61	23.64	3.767	130	29	48	46.91	46.91	1.937	246	4	4
23.66		3.761	112	37		47.16	47.16	1.927	424	2	8
24.22	24.22	3.675	200	3	4	47.16		1.927	424	10	
24.51	24.51	3.631	130	23	20	48.36	48.38	1.882	352	2	
24.61		3.618	132	5		48.41	48.41	1.880	224	6	7
25.69	25.69	3.468	114	3	3	49.17	49.37	1.853	352	2	8
26.52	26.52	3.360	114	8	7	49.37		1.846	406	11	
27.45	27.45	3.249	220	29	27	49.57		1.839	064	2	
27.80	27.82	3.209	040	84	93	49.61	49.60	1.838	400	11	10
27.91	27.91	3.197	204	86	100	49.66		1.836	116	2	
28.04	28.04	3.181	004	86	85	50.25	50.25	1.816	260	6	4
28.49	28.49	3.132	220	23	21	50.45	50.43	1.809	264	2	3
29.42	29.42	3.036	132	12	10	50.78	50.78	1.798	116	8	8
30.26	30.26	2.954	042	17	15	50.81		1.797	170	4	
30.43	30.43	2.938	024	16	14	51.12	51.16	1.787	420	2	3
30.78	30.78	2.905	224	9	7	51.33	51.33	1.780	172	2	3
31.59	31.59	2.832	132	7	5	51.64	51.64	1.770	208	18	11
31.81	31.81	2.813	134	4	4	52.00	52.00	1.759	244	8	6
32.10	32.12	2.788	221	1	2	52.33		1.748	264	1	
33.06	33.06	2.709	202	2	1	52.37	52.38	1.747	420	2	4
33.84	33.84	2.649	134	4	3	52.42		1.745	172	1	
35.14	35.14	2.554	222	3	3	52.80	52.80	1.734	228	3	4
35.73	35.73	2.513	242	2	19	52.81		1.734	136	2	
35.73		2.513	242	7		53.33	53.33	1.718	064	3	3
35.91	35.88	2.501	314	9	10	53.60	53.60	1.710	444	7	9
36.38	36.38	2.469	240	8	10	53.61		1.710	444	6	
36.53		2.459	114	13		54.62	54.62	1.680	228	3	2
36.59	36.56	2.456	150	12	17	55.64	55.64	1.652	244	6	3
36.80		2.442	222	2		56.58	56.58	1.627	338	1	2
37.26	37.26	2.413	152	5	4	57.10	57.04	1.615	446	1	1
37.60	37.60	2.392	150	9	7	57.44	57.44	1.604	080	3	2
38.00	38.00	2.368	240	13	9	57.97	57.97	1.591	008	1	1
38.35	38.35	2.347	044	2	3	58.27	58.27	1.583	082	2	2
38.69	38.69	2.327	315	1	2	58.76	58.76	1.571	028	2	2
38.95	39.00	2.312	362	3	5	59.03	59.03	1.564	428	2	2
39.03		2.308	244	4		60.26	60.10	1.536	266	1	2
39.53	39.53	2.280	332	12	9	61.34	61.36	1.511	248	3	2
39.81	39.81	2.264	116	10	8	62.14		1.494	280	3	
40.43	40.43	2.230	226	2	2	62.26	62.26	1.491	282	5	5
40.56	40.54	2.224	244	2	2	62.32		1.490	176	1	
41.40	41.40	2.181	334	3	3	62.56	62.56	1.485	462	4	3
41.92	41.94	2.155	226	2	3	62.72	62.72	1.481	536	3	3
42.25	42.28	2.139	060	6	19	62.94		1.477	084	1	
42.29		2.137	242	24		63.32	63.32	1.469	464	1	4
						64.04	64.04	1.454	066	3	3
						64.33	64.34	1.448	280	2	3
						64.35		1.448	246	3	

TABLE 6. CALCULATED POWDER DATA FOR ANORTHITE (An₁₀₀)

2θ(INT)	2θ(P)	d	hkl	I _{INT}	I _P	2θ(INT)	2θ(P)	d	hkl	I _{INT}	I _P
13.01	13.01	6.807	111	9	8	45.22	45.20	2.005	312	3	4
13.58	13.58	6.522	110	10	8	45.54	45.54	1.992	136	3	3
13.79	13.79	6.420	020	4	4	45.69	45.68	1.986	062	4	4
17.33	17.32	5.118	111	3	2	46.16	46.14	1.966	312	3	4
17.73	17.73	5.002	121	2	1	46.38	46.38	1.958	224	3	3
18.92	18.92	4.690	022	17	14	47.04	47.04	1.932	424	11	9
20.95	20.95	4.240	003	2	2	47.32	47.32	1.921	424	5	4
22.01	22.01	4.039	202	58	48	48.10		1.892	352	2	4
22.71	22.71	3.916	112	13	11	48.11	48.10	1.891	260	4	
23.52		3.783	130	30	28	48.47	48.47	1.878	224	9	7
23.62	23.52	3.767	131	5		49.27		1.849	353	2	
23.69	23.68	3.756	112	17	19	49.39	49.42	1.845	246	2	12
24.59		3.620	130	38	33	49.41		1.845	406	11	
24.71	24.60	3.603	132	13		49.61		1.838	064	3	
25.37	25.37	3.510	132	4	4	49.62	49.62	1.837	400	18	16
25.63		3.476	131	4	14	49.69		1.835	116	4	
25.75	25.76	3.459	114	15		50.42	50.44	1.810	260	5	5
26.18	26.18	3.403	222	7	7	50.67	50.68	1.802	264	5	8
26.51	26.51	3.362	114	31	25	50.68		1.801	170	4	
27.35	27.35	3.261	220	64	52	50.81	50.81	1.797	116	10	9
27.79	27.79	3.210	040	53	63	51.69	51.69	1.768	208	26	17
27.93	27.93	3.194	204	100	100	51.91	51.88	1.761	244	8	8
28.06	28.06	3.180	004	93	91	52.27	52.26	1.750	172	3	4
28.59	28.59	3.122	220	49	39	52.58	52.52	1.742	154	3	4
29.36	29.36	3.042	132	23	18	52.67		1.738	262	3	
30.27	30.27	2.952	042	33	27	52.92	52.82	1.733	442	4	6
30.46	30.46	2.934	024	20	19	52.93		1.730	228	3	
30.91	30.92	2.893	224	8	8	53.28		1.719	064	4	
31.64	31.64	2.828	132	27	20	53.35	53.34	1.717	444	4	7
31.92	31.92	2.804	134	11	9	53.48		1.713	046	3	
33.76	33.76	2.655	134	18	14	53.87	53.88	1.702	444	6	5
35.07	35.07	2.559	222	5	6	54.59	54.58	1.681	228	5	4
35.50		2.529	114	7	20	55.73	55.73	1.649	244	3	2
35.55	35.54	2.525	242	22		56.94	56.94	1.617	356	5	4
35.79		2.509	314	4	28	57.41	57.38	1.605	080	3	3
35.91	35.90	2.501	242	37		58.83	58.83	1.570	028	3	3
36.88		2.437	222	5	6	59.35	59.32	1.557	334	3	3
37.01	36.88	2.429	310	3		59.61	59.61	1.551	319	3	3
37.37	37.37	2.406	152	5	4	60.09		1.540	428	2	
37.73	37.72	2.384	310	3	4	60.22	60.26	1.537	534	2	4
38.13		2.360	152	3	5	60.27		1.536	352	4	
38.14	38.14	2.359	240	3		60.91		1.521	264	2	
38.77	38.78	2.323	332	9	8	61.04	61.06	1.518	028	2	4
39.25	39.25	2.295	153	3	3	61.05		1.518	119	2	
39.71		2.270	332	6	7	61.08		1.517	534	2	
39.82	39.72	2.264	116	5		61.23		1.514	248	2	
40.28		2.239	152	5	4	61.90	61.90	1.499	280	7	5
40.39	40.28	2.233	244	3		62.22	62.22	1.492	462	7	6
41.85	41.85	2.158	226	4	4	62.47	62.48	1.487	282	6	6
42.16		2.143	242	19	17	62.40		1.486	334	2	
42.23	42.18	2.140	060	10		62.94		1.477	536	3	
42.69	42.69	2.118	245	3	4	62.97	62.96	1.476	084	2	10
43.17	43.17	2.095	162	14	10	62.97		1.476	464	6	
43.79	43.79	2.067	045	3	3	62.98		1.476	536	4	
44.75	44.75	2.025	164	3	3	62.99		1.476	532	1	
44.88		2.019	404	3	5	64.00	64.00	1.455	066	9	5
44.96	44.94	2.016	402	5		64.30	64.30	1.449	246	4	3
						64.51	64.51	1.444	280	3	3

TABLE 7. "c" AND "d" REFLECTIONS IN ANORTHITE (AN₁₀₀)

2θ (INT)	d	hkl	I_{INT}	2θ (INT)	d	hkl	I_{INT}
6.95	12.718	001	0.6	29.17	3.061	041	1.1
13.01	6.807	$\bar{1}\bar{1}1$	9.0	30.60	2.921	221	0.6
15.00	5.904	0 $\bar{2}$ 1	1.2	30.96	2.889	140	0.6
15.10	5.869	0 $\bar{1}$ 2	0.6	32.10	2.781	221	2.1
15.90	5.573	021	0.7	32.90	2.723	$\bar{2}$ 05	1.8
17.33	5.118	$\bar{1}\bar{1}1$	2.6	33.79	2.653	043	1.7
19.32	4.594	$\bar{1}\bar{2}$ 2	1.1	34.23	2.620	$\bar{1}$ 33	0.6
19.96	4.448	$\bar{1}\bar{1}$ 3	1.1	35.11	2.556	$\bar{3}$ 11	2.1
20.58	4.316	$\bar{1}$ 13	0.7	35.28	2.544	005	0.5
20.95	4.240	003	2.4	35.29	2.543	$\bar{2}$ 25	1.8
23.42	3.798	$\bar{1}$ 31	0.8	36.34	2.472	225	1.4
23.62	3.767	$\bar{1}$ 31	5.0	36.83	2.440	$\bar{1}$ 51	1.3
24.12	3.689	203	1.5	36.90	2.436	$\bar{2}$ 43	0.6
24.31	3.661	023	0.9	37.73	2.384	$\bar{1}$ 51	1.1
25.63	3.476	$\bar{1}$ 31	4.4	38.78	2.322	$\bar{3}$ 15	1.5
26.00	3.426	023	1.2	39.01	2.301	025	1.9
27.42	3.253	131	0.6	39.25	2.295	$\bar{1}$ 53	2.7
27.63	3.229	$\bar{1}$ 33	1.5	39.51	2.280	331	0.9
27.75	3.215	$\bar{2}$ 23	1.0	39.72	2.269	$\bar{3}$ 33	0.8
28.88	3.092	$\bar{1}$ 13	0.7				

Thus, profiles of observed peaks are convolutions of the X-ray spectral distribution and are strongly influenced by instrumental aberrations, sample alignment, and effects that relate to particle size, strain and homogeneity of the sample. Thus, the calculated peak intensities reflect assumptions that have been made concerning the shape of the diffraction maxima as well as overlap of adjacent maxima. They are: (1) the diffraction maxima from both $K\alpha_1$ and $K\alpha_2$ have Cauchy profiles; (2) the width of the profile at half maximum is dependent on the diffraction angle and can be estimated without evaluating the individual factors mentioned above which influence it; (3) adjacent maxima will overlap to produce a single I_P when separated by less than one half-width.

The relation of half-width to 2θ in (2) is based on empirical data from α -Al₂O₃ and Si. The data were measured on diffractometer traces of uncemented powders in standard holders, using a Norelco wide-angle goniometer over the whole 2θ range ($1/4^\circ$ 2θ . min scan using a pulse-height analyzer, 1° divergent and scattering slits and 0.003 in. receiving slits). The half-widths recorded on Al₂O₃ and Si are more narrow (0.10° at $2\theta=40^\circ$) than recorded in plagioclase scanned under similar conditions (0.10 – 0.16° at $2\theta=40^\circ$). This is due in large part to the greater compositional variation in samples of natural silicates. The I_P data of Tables 2–7 are based on the half-width versus 2θ function determined on Al₂O₃ and Si extrapolated to a half-width of 0.16° at 40° 2θ .

The intensities I_{INT} and I_P (Tables 2–7) are directly related to intensities obtained from diffractometry which utilizes flat samples and thus eliminates absorption corrections for materials with moderate absorption. Use of cylindrical samples in Debye-Scherrer cameras requires an absorption correction; and within the angular range reported, the resultant I_{INT} and I_P differ so slightly from those tabulated for flat samples (see Table 8) that they have not been included in Table 2–7. In general, absorption in cylindrical mounts causes the front reflection to be relatively weaker than the back reflection region, the effect being pronounced in compounds containing the heavier elements.

TABLE 8. EXAMPLES OF INTEGRATED INTENSITIES IN ANORTHITE FOR CYLINDRICAL (C) AND FLAT SAMPLES (F)

hkl	2θ CuK α (deg)	$I_{INT}(F)$	$I_{INT}(C)$
111	13.01	9.0	7.9
202	22.01	58.3	54.9
204	27.93	100.0	100.0
152	43.17	14.0	16.7
066	64.00	8.8	13.5

In the case of calculated integrated intensities (I_{INT}), the strongest peak was set to 100 (002 for albite and oligoclase; $\bar{2}02$ and $\bar{2}04$ for bytownite and anorthite, respectively). Peak intensities (I_P), graphically displayed in Figures 1-4 and also included in Tables 2-6, are scaled to the maximum observed which was set at 100.

In view of the relatively narrow spectra of spacings, normally measured and indexed in these complex powder patterns, an unresolved CuK α radiation was used in the computations. The total number of reflections that could be calculated was limited by the code to 1000, thus restricting the maximum 2θ angle to 87° for C-centered cells and to 65° for primitive and body-centered cells. However, in consideration of space limitations, only those hkl reflections whose calculated integrated

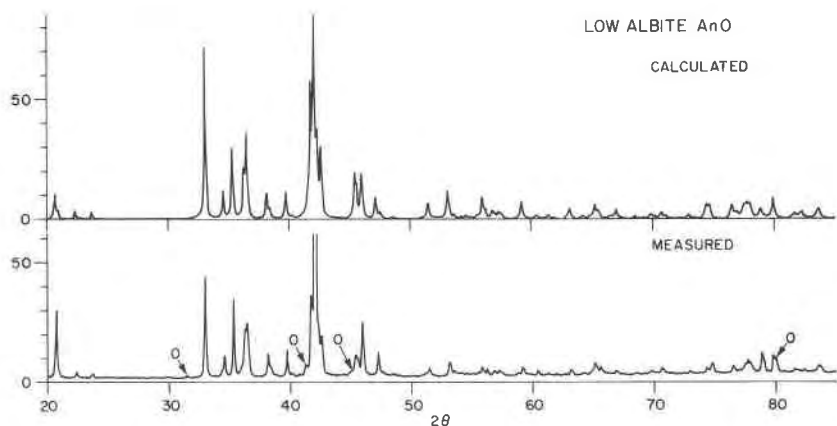


FIG. 1. Powder patterns at low albite, CrK α . (a) Calculated pattern of Ramona albite, (b) measured pattern of Amelia albite by William Parrish, Phillips Laboratories. Peaks marked "O" are due to impurities. (40 kVp/20mA, 10° take-off angle on point source, vacuum diffractometer, $\frac{1}{2}^\circ$ /min, time const = 2 sec, $2-\frac{1}{2}^\circ$ angular aperture, 0.006 in. (0.05°) receiving slit, specimen rotated in its own plane.)

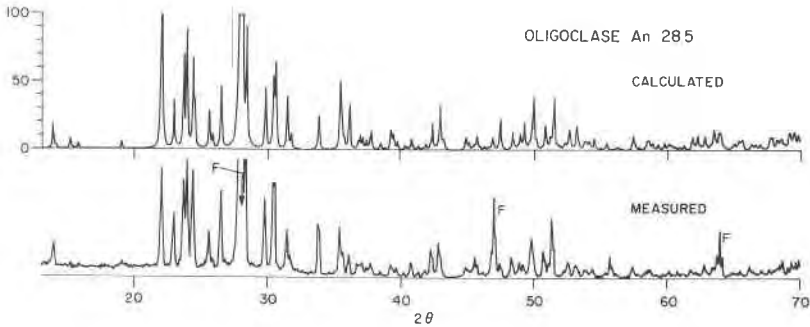


FIG. 2. Powder patterns of oligoclase, An_{29} , Mitchell Co., N.C., $CuK\alpha$. (a) Calculated pattern, (b) measured pattern by D. B. Stewart, U.S.G.S. F=fluorite. (45kVp/20mA, 1° /min, time const=4 sec, 1° divergent and anti-scatter slits, 0.006 in. receiving slit, pulse height analyzer.)

intensities met the following criteria were included in Tables 2-6:¹ $100I_{hkl}/I_{002} > 2.4$ (albite and oligoclase); $100I_{hkl}/I_{202} > 1.4$ (bytownite); and $100I_{hkl}/I_{204} > 2.4$ for $2\theta = 0^\circ-60^\circ$ and > 1.4 for $2\theta = 61^\circ-65^\circ$ (anorthite). In consideration of the importance of weak "c" reflections ($h+k$, even; l , odd) in distinguishing anorthite and transitional anorthite, a separate Table 7 lists "c" and "d" reflections ($h+k$, even; l odd and $h+k$,

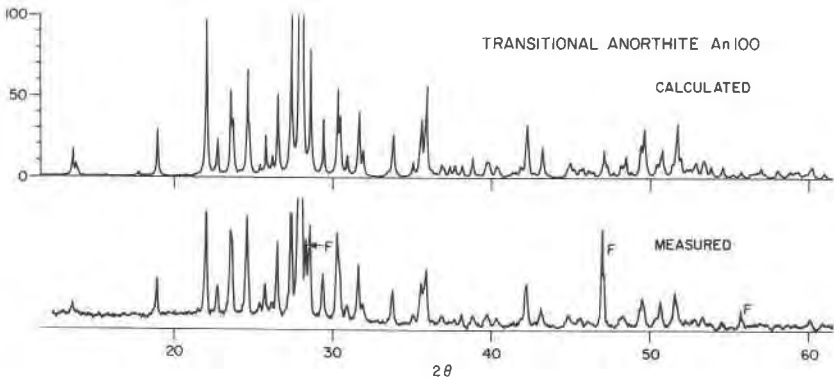


FIG. 3. Powder patterns of synthetic transitional anorthite, An_{100} , ANS-26 (Stewart, 1967, p. 50), $CuK\alpha$. (a) Calculated pattern, (b) measured pattern by D. B. Stewart, U.S.G.S. F=fluorite. (Experimental conditions as in Fig. 2b.)

¹ 20 receive unabridged Tables 2-6, order NAPS Document-00038 from ASIS National Auxiliary Publications Service, c/o CCM Information Sciences, Inc., 22 West 34th Street, New York, N. Y. 10001; remitting \$2.00 for microfiche or \$6.00 for photocopies.

odd; l , even respectively) for anorthite. Most are too weak to be included in Table 6. Criterion for inclusion in Table 7 is $100I_{hkl}/I_{204} > 0.05$ and $2\theta < 40^\circ$.

RESULTS AND CONCLUSIONS

Calculated diffractometer traces are juxtaposed with real diffractometer traces in Figures 1–4 to illustrate their generally good agreement. Except for Figure 1, real traces are measured on smear mounts; no effort was made to eliminate preferred orientation in any of the four.

The calculated traces in Figures 1–4 are based on an assumed half-width at $40^\circ 2\theta$ of 0.12–0.13° which is smaller than that used to calculate

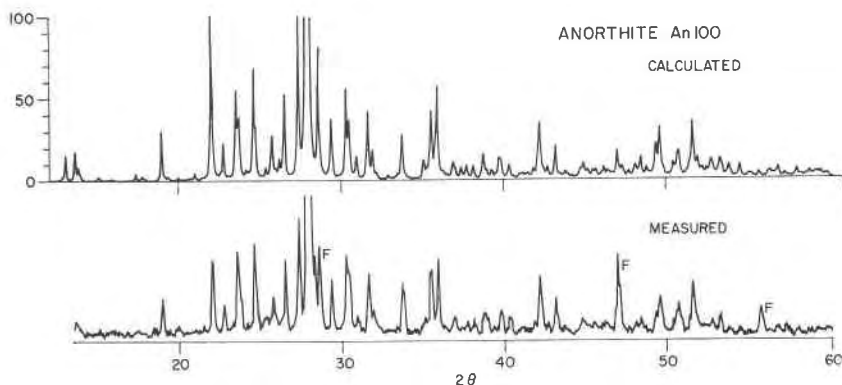


FIG. 4. Powder patterns of synthetic anorthite, An_{100} , ANS-305 (Stewart, 1967, p. 50), $CuK\alpha$. (a) Calculated pattern, (b) measured pattern by D. B. Stewart. F=fluorite (experimental conditions as in Fig 2b).

the I_P of Tables 2–7 (0.16°). Use of the smaller value was necessary in order to match the good resolution in the real patterns. These are not only of high quality but also include traces from synthetic plagioclases. In contrast to the natural plagioclases, the latter are more uniform in composition and therefore also in unit cell size; as a consequence, line broadening from these sources is not expected. The 0.16° half-width used for calculated I_P in the Tables and Figure 5 is considered to be a better approximation for natural plagioclases. But even use of the large half-width results in plots with resolution that may not be found in natural patterns. For example, in the high albite trace (Fig. 5), resolution of 041 , 022 , and $\bar{2}22$ at $2\theta \sim 30.5$ and 131 and $\bar{1}\bar{3}2$ at $2\theta \sim 31.7^\circ$ has no counterpart in the measured patterns recorded in Figure 1 (Smith and Yoder, 1956) and Figure 1 (Bambauer *et al.*, 1967). The lack of resolution may reflect incorrect overlap criterion used in the calculated

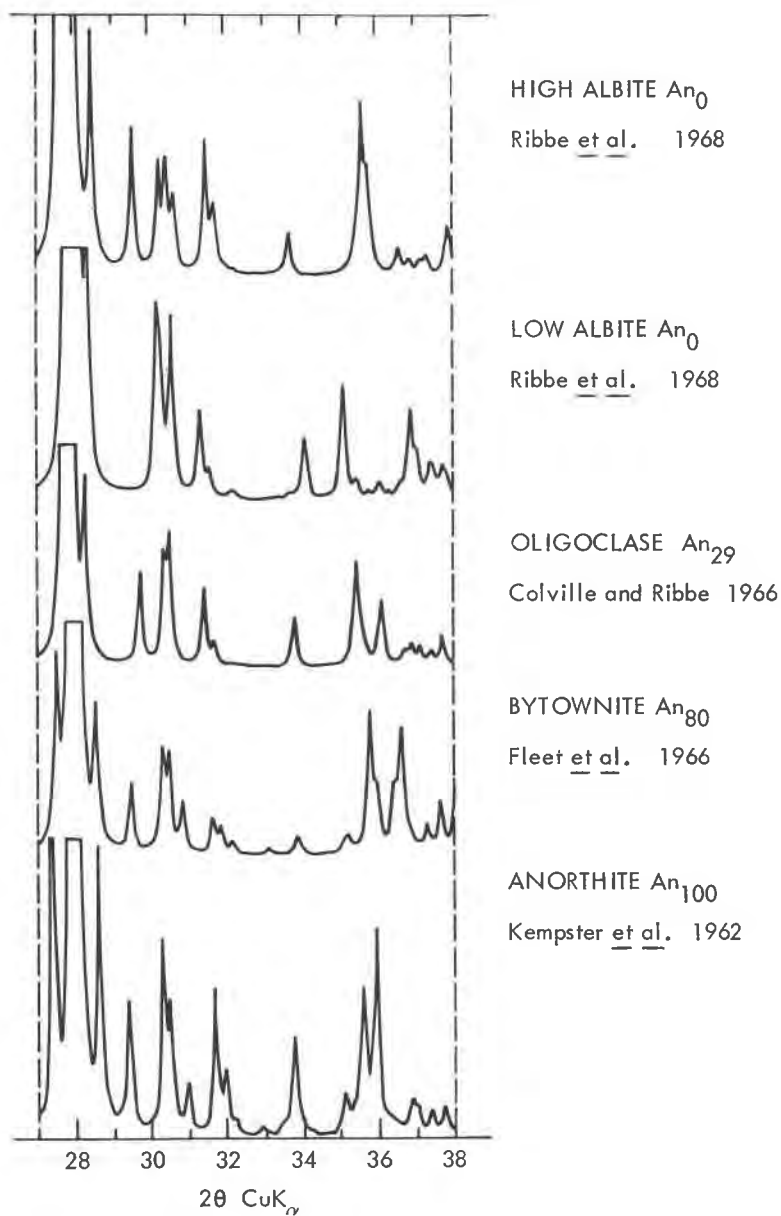


FIG. 5. Portions of calculated powder patterns.

model, which is determined by the half-width chosen, or slight differences in lattice parameters in the various plagioclases used.

The chief differences in the juxtaposed patterns is in the intensities of certain peaks. For example, in real traces of oligoclase, anorthite and transitional anorthite (Figs. 2-4), the $\bar{2}0l$ peaks at $2\theta \cong 22.0^\circ$ are low relative to the calculated counterpart. The reasons for these differences are not certainly known, but are believed to be due to a preferred orientation of the particles on the slide mounts because of perfect (001) and (010) cleavages. Under these circumstances, lower intensities of $h00$, $h0l$ and hkl peaks would be anticipated as well as enhancement of $00l$, $0k0$ and $0kl$. In our experience, peak heights in synthetic materials, more closely resemble the calculated than do those in natural minerals. The observation is in keeping with an initial finer grain size in synthetics, which eliminates the need for further grinding and therefore the production of particles bounded by cleavages.

It is hoped that the calculated integrated and peak intensities presented here will serve as guides to indexing the complex patterns of the plagioclases. If so, the data will have helped to eliminate one important source of error in the process of reducing powder data to meaningful parameters, *vis.*, mis-identification of diffraction maxima.

For indexing complex patterns, we recommend use of the calculated I_{INT} and I_{P} of Tables 2-7 to recognize overlap, and in such cases to assess the likely contribution of each reflection to the observed peak maximum. As is well-known, overlap of a strong and a weak reflection can result in a single peak whose intensity is enhanced as well as skewed off the 2θ value associated with the stronger of the two. In the case where the ratio of the intensities is large, *e.g.* 10:1, the peak can be confidently associated with the hkl of the stronger, but if the ratio approaches 1:1 and the reflections do not exactly coincide, the d of the peak does not correspond to either reflection. Even in the case of closely spaced, but resolved reflections, the position of each is effected to some extent by proximity of the other. These considerations put a limit on the ultimate accuracy of lattice parameters calculated by least-square refinements of triclinic powder data assuming otherwise ideal conditions.

In resumé, I_{P} in calculated as well as measured powder patterns must be interpreted with discretion. These intensities are influenced by overlap of maxima and by line-broadening related to minor variations in sample, composition, particle size, instrumental aberrations, strain, and sample alignment. In addition, preferred orientation, because of perfect cleavages and dimensional alignment of particles, is a factor that influences I_{P} . Nonetheless, the data presented here make reasonable al-

lowance for many of these variables, and by doing so simulate natural patterns.

ACKNOWLEDGMENTS

We are grateful to Paul Ribbe, A. Colville, Helen Megaw, and W. H. Taylor for making the results of their structure analyses available before publication. Comment and recommendations by D. B. Stewart and Helen Megaw have greatly improved the lucidity of the text. Finally, we are in debt to D. B. Stewart and W. Parrish for their high-quality diffractometry data on natural plagioclases which were used in the illustrations.

Work performed under the auspices of the U. S. Atomic Energy Commission.

REFERENCES

- BAMBAUER, H. U., M. CORLETT, E. EBERHARD AND K. VISWANATHAN (1967) Diagrams for the determination of plagioclase using X-ray powder methods. Part III. *Schweiz. Mineral. Petrog. Mitt.*, **47**, 333-349.
- COLE, W. F., H. SORUM AND W. H. TAYLOR (1951) The structures of plagioclase feldspars. I. *Acta Crystallogr.*, **4**, 20-29.
- COLVILLE, A. A., AND P. H. RIBBE (1966) The crystal structure of oligoclase. (abstr.) *Geol. Soc. Amer. Spec. Pap.*, **101**, 41.
- FERGUSON, R. B., R. V. TRAILL AND W. H. TAYLOR (1958) The crystal structures of low-temperature and high-temperature albites. *Acta Crystallogr.*, **11**, 331-348.
- FLEET, S. G., S. CHANDRASEKHAR, AND HELEN D. MEGAW (1966) The structure of bytownite ('body-centered anorthite'). *Acta Crystallogr.*, **21**, 782-801.
- KEMPSTER, C. J. E., HELEN D. MEGAW, AND E. W. RADOSLOVICH (1962) The structure of anorthite, $\text{CaAl}_2\text{Si}_2\text{O}_8$. I. Structure analysis. *Acta Crystallogr.*, **15**, 1005-1017.
- MEGAW, HELEN D., C. J. E. KEMPSTER, AND E. W. RADOSLOVICH (1962) The structure of anorthite, $\text{CaAl}_2\text{Si}_2\text{O}_8$. II. Description and discussion. *Acta Crystallogr.*, **15**, 1017-1035.
- RIBBE, P. H., AND HELEN D. MEGAW (1963) The structure of transitional anorthite. A comparison with primitive anorthite. *Norsk Geol. Tids.*, **42**, 158-167.
- , ———, AND W. H. TAYLOR (1968) The albite structure. *Acta Crystallogr.* (in press).
- SMITH, D. K. (1968) Computer simulation of X-ray diffractometer traces. *Norelco Rep.*, **15**, 57-65.
- (1967) A revised program for calculating X-ray powder diffraction patterns. Lawrence Rad. Lab. [*U. S. Clearinghouse Fed. Sci. Tech. Inform.*]UCRL-50264.
- SMITH, J. R., AND H. S. YODER (1956) Variations in X-ray powder diffraction patterns of plagioclase feldspars. *Amer. Mineral.*, **41**, 632-647.
- STEWART, D. B. (1967) Four-phase curve in the system $\text{CaAl}_2\text{Si}_2\text{O}_8\text{-SiO}_2\text{-H}_2\text{O}$ between 1 and 10 kb. *Schweiz. Mineral. Petrog. Mitt.*, **47**, 35-59.

Manuscript received, December 6, 1967; accepted for publication, March 17, 1968.